Quantitative Finance and Economics

http://www.aimspress.com/journal/QFE

QFE, 6(1): 138–157.
DOI: 10.3934/QFE.2022006
Received: 03 March 2022
Revised: 27 March 2022
Accepted: 28 March 2022
Published: 30 March 2022

Research article

Longevity risk analysis: applications to the Italian regional data

Salvatore Scognamiglio*

Department of Management and Quantitative Sciences, University of Naples "Parthenope", Naples, Italy

* **Correspondence:** Email: salvatore.scognamiglio@uniparthenope.it.

Abstract: Longevity risk is the risk that members of a given population will live longer than expected. When it occurs, pension providers may have to pay pensions for longer than expected, significantly increasing their costs. While this risk is being adequately studied using the national mortality data provided by the Human Mortality Database, relatively few studies exist that analyse sub-national data. This manuscript proposes a comparative study of some stochastic mortality models to measure the longevity risk on Italian mortality data at the regional level. In particular, the use of the Lee-Carter and Li-Lee models is explored. The models are compared in fitting quality, forecasting accuracy and complexity. Numerical experiments and applications to immediate life annuity evaluation are presented.

Keywords: mortality modelling; multi-population mortality modelling; risk analysis; Lee–Carter model; time series forecasting

JEL Codes: C02, C15, C22

1. Introduction

In recent decades, life expectancy has been increasing in the most developed countries, mainly thanks to the improvements in nutrition, hygiene, medical technology, health care, lifestyle. EUROSTAT statistics show that the life expectancy for an individual aged 65 over the last 30 years is increased in almost all European countries (27% in Italy, 28% in Spain and 25% in Greece). These improvements, which are generally perceived as positive by individuals, have effects on retirement costs pose significant challenges for governments as well as for individual pension funds and life insurers as described in De Waegenaere et al. (2010). For example, we consider the savings needed to finance a stream of pensions consumption that pays 1 per year. The expected present value of such annuity for an Italian individual aged 65 (with an interest rate equal to 0) increased from 17.2 in 1990 to 21.8 in 2020. Pension providers and actuaries should consider these longevity improvements in life insurance pricing and reserving to avoid underestimating their future liabilities.

There is extensive literature on mortality forecasting, especially in the category of extrapolation methods, see for example Renshaw & Haberman (2003); Currie et al. (2004); Cairns et al. (2006, 2009). The model proposed by Lee & Carter (1992) (LC) is the best-known approach to stochastically model and forecast the mortality rates of a given population. Their model decomposes the age-time matrix of mortality rates into a bi-linear combination of age and period parameters using the Principal Component Analysis (PCA). Forecasting is performed by projecting the time-index component into the future with time-series models. A formal description of the LC model is presented in the next section. The literature is rich in contributions that extended it in different directions or developed different models. Brouhns et al. (2002) proposed an alternative to the Ordinary Least Squared estimation approach of the classical LC method by assuming the Poisson distribution for the number of deaths and employing maximum likelihood for parameter estimation. Renshaw & Haberman (2003) explored multi-factor extensions of the LC model, while Renshaw & Haberman (2006) suggested the incorporation of a cohort effect. Other extensions of the LC model can be found in Currie (2013); Nigri et al. (2019); Gao & Shi (2021). Another very popular mortality model is the Cairns Blake Dowd (CBD) model proposed in Cairns et al. (2006). It proceeds by fitting a parametric mortality model to each calendar year of mortality experience separately and then extrapolating the coefficients to future years with time series models. Many extensions of the CBD model have been proposed and investigated. Cairns et al. (2009) presented some of them augmenting the classical CBD with a quadratic component in the parametric model or a cohort effect. Hyndman & Ullah (2007) introduced a functional data approach in which the mortality data of each year are smoothed via constrained regression splines before fitting a model using principal components decomposition, and Hainaut & Denuit (2020) further extended the idea suggesting a wavelet-based decomposition. Despite the numerous contributions, the LC model is extensively used by practitioners and academics thanks to its simplicity and discrete forecasting accuracy.

Enchev et al. (2017) remarks that the drivers of the longevity improvements mentioned above often spread quickly, and the mortality of different populations appears, in some way, correlated. For instance, adverse events such as pandemics or wars can have a transversal impact on the mortality rates of many countries. For this reason, the study of models able to describe the mortality dynamics of multiple populations has aroused interest in recent years. Populations can differ for various features such as gender, country or geographical area. One of the most straightforward approaches for multi-population mortality modelling consists of using a set of independent models. Single-population mortality models, e.g. LC models, are applied to the considered populations individually, and an own model describes the mortality of each population. However, this approach completely ignores the dependency among mortality of the different populations. Some authors address this issue by introducing common terms in the single-population models. A very popular model is the (Augmented) Common Factor model developed in Li & Lee (2005) that proposes a double log-bilinear mortality model augmenting common age and period effects with sub–population-specific age and period effects. An attractive property of this model is producing "coherent mortality forecasts" in that it ensures that long-term forecasts do not diverge among the populations. A Poisson version of the Augmented Common Factor model is proposed in Li (2013). In contrast, Kleinow (2015) relaxes the coherence assumption by imposing that only the age-specific LC parameters modulate the period effect are common to all populations. At the same time, different time indices fit each population. Other examples of multi-population mortality models can be found in Hyndman et al. (2013); Schnürch et al. (2021); Chen et al. (2015). While multi-population mortality models for populations belonging to different countries or genders have been

extensively investigated at the country level, few studies exist that analyse sub-national and regional mortality data. A recent application of multi-population models to United Kingdom data can be found in Chen & Millossovich (2018), while Shang & Yang (2021) analyses the Australian sub-national data. One of the few studies that analyse sub-national Italian data is presented in Danesi et al. (2004), where a comparison of some single-population models is discussed. This manuscript proposes a comparative study between single-population and multi-population mortality models on Italian mortality data at the regional level. Italy represents an interesting case study for some reasons. On the one hand, the differences among the Italian regions (in terms of socio-economic development, living conditions, and historical differences), particularly between those located in the north and south of the country, represent a longstanding issue and is currently highly debated in the literature, see for example Franzini L & Giannoni M (2010). It is reasonable to think that these differences could induce differences in mortality among populations living in the different Italian areas. On the other hand, all the Italian regions share the same regulatory, political, and health systems, which induces a somewhat dependency structure among the regional mortality rates. The application of single-population LC models and the Li and Lee Model is analysed. The comparison appears interesting since both models adopt a linear structure for the time component. However, the approach based on single-population LC models assumes total independence among the mortality of the different regions, while the Li and Lee model assumes that a single factor drives the mortality of the different regions and only short-term divergences are allowed.

The remainder of the paper is organised as follows. Section 2 provides a formal description of the mortality models considered; Section 3 describes the numerical experiments and the results, Section 4 shows an application to the life annuities pricing, and Section 5 concludes.

2. Materials and methods

This section introduces the stochastic mortality models used in this research. We denote by $\mathcal{X} = \{x_0, x_1, \ldots, x_\omega\}$ the set of the age categories, $\mathcal{T} = \{t_0, t_1, \ldots, t_n\}$ the set of calendar years considered and $\mathcal{I} = \{\mathsf{pop}_1, \mathsf{pop}_2, \ldots, \mathsf{pop}_m\}$ the set of sub-population considered.

2.1. Independent modelling

The LC model is the most popular approach to model the mortality of a single population. It specifies a log-bilinear form for the logarithm of the central death rate $\log m_{x,t} \in \mathbb{R}$ at age $x \in \mathcal{X}$ in the year $t \in \mathcal{T}$ in a given population:

$$\log(m_{x,t}) = \alpha_x + \beta_x \kappa_t + \epsilon_{x,t}, \qquad \textit{with i.i.d } \epsilon_{x,t} \sim N(0, \sigma_\epsilon^2) \tag{1}$$

where $\alpha_x \in \mathbb{R}$ describes the average pattern of mortality for the age group; $\beta_x \in \mathbb{R}$ represents the age-specific patterns of mortality change, indicating the sensitivity of the logarithm of the force of mortality at age x to variations in the time index κ_t; $\kappa_t \in \mathbb{R}$ explains the time trend of the general mortality level; and $\epsilon_{x,t}$ represents the deviation of the model from the observed log-central death rate. To avoid identifiability problems, the authors suggest imposing the following constraints

$$\sum_{x \in \mathcal{X}} \beta_x = 1 \qquad \sum_{t \in \mathcal{T}} \frac{\kappa_t}{|\mathcal{T}|} = 0 \tag{2}$$

The estimates of the LC parameters are obtained by solving the optimisation problem

$$\underset{(\alpha_x)_x,(\beta_x)_x,(\kappa_t)_t}{\arg\min} \sum_{x\in\mathcal{X}} \sum_{t\in\mathcal{T}} \Big(\log(m_{x,t}) - \alpha_x - \beta_x\kappa_t \Big)^2 \tag{3}$$

$(\alpha_x)_x$* are estimated as the logarithm of the geometric mean of the crude mortality rates, averaged over all t, for each $x \in \mathcal{X}$

$$\hat{\alpha}_x = \log\Big(\prod_{t\in\mathcal{T}} (m_{x,t})^{1/|\mathcal{T}|} \Big)$$

while $(\kappa_t)_t$ and $(\beta_x)_x$ are estimated using a first-order Singular Value Decompotion (SVD) to the center log-mortality matrix $H = \{h_{x,t}\}_{x\in\mathcal{X},t\in\mathcal{T}} \in \mathbb{R}^{|\mathcal{X}|\times|\mathcal{T}|}$ where

$$h_{x,t} = \big(\log(m_{x,t}) - \hat{\alpha}_x \big)$$

To forecast future mortality rates, the model assumes that the α_x and β_x parameters remain constant over time and forecast future values of k_t using a standard univariate time series model. Despite several ARIMA (p, d, q) models could be considered, in practice the random walk with drift model is used almost exclusively:

$$\kappa_t = \kappa_{t-1} + \gamma + \xi_t \qquad with\ i.i.d\ \xi_t \sim N(0, \sigma^2_\xi) \tag{4}$$

where $\gamma \in \mathbb{R}$ is the drift. When the aim is to model and forecast the mortality of many different sub-populations $\forall i \in \mathcal{I}$, one could apply an LC model for each subgroup considered. In this setting, the mortality of each sub-group is described independently from the others. The model reads:

$$log(m^{(i)}_{x,t}) = \alpha^{(i)}_x + \beta^{(i)}_x \kappa^{(i)}_t + \epsilon^{(i)}_{x,t} \qquad \forall i \in \mathcal{I} \tag{5}$$

The model fitting is performed individually $\forall i \in \mathcal{I}$ and the population-specific time indices $\kappa^{(i)}_t$ are projected with independent ARIMA (0,1,0) models.

2.2. Coherent Mortality modelling

Applying independent LC models to multiple populations can produce divergent long-term predictions. However, if two or more populations share similar socioeconomic conditions, it might be reasonable to assume that the differences in mortality among them should not diverge over time.

To avoid long-run divergence, Li & Lee (2005) proposed a model where all the populations share the parameters of the bilinear term ($\beta^{(i)}_x = B_x \in \mathbb{R}$ and $\kappa^{(i)}_t = K_t \in \mathbb{R}, \forall i \in I$). They define the Common Factor (CF) model as:

$$\log m^{(i)}_{x,t} = \alpha^{(i)}_x + B_x K_t + \nu^{(i)}_{x,t}, \qquad with\ i.i.d\ \nu^{(i)}_t \sim N(0, (\sigma^{(i)}_\nu)^2) \tag{6}$$

where K_t is a common risk factor shaping all populations' mortality evolution, which is modulated by the age-specific parameter B_x and ν is the normally distributed error term. While the $\alpha^{(i)}_x$ is estimated separately for each individual sub-population, the estimates of B_x and K_t are obtained by applying

* The notation $(\alpha^{(i)}_x)_x$ indicates the curve of the α_x for the different ages x parameters of a given population i. The same notation is used in the following also for the other parameters.

the ordinary LC method to the whole group. The time-specific common factor K_t is a non-stationary process, and a random walk with drift model is used to obtain forecasts:

$$K_t = K_{t-1} + \delta + \eta_t \qquad with\ i.i.d\ \eta_t \sim N(0, (\sigma_\eta^{(i)})^2) \tag{7}$$

To improve the fitting and forecasting, the authors suggest to include in the CF model an additional bilinear term with population-specific parameters. In that case, we obtain the Augmented Common Factor (ACF) Model:

$$\log m_{x,t}^{(i)} = \alpha_x^{(i)} + B_x K_t + b_x^{(i)} k_t^{(i)} + \zeta_{x,t}^{(i)}, \qquad with\ i.i.d\ \zeta_t^{(i)} \sim N(0, (\sigma_\zeta^{(i)})^2) \tag{8}$$

where the estimates of $b_x^{(i)}$ and $k_t^{(i)}$ are obtained by applying the first-order SVD to the residuals matrix of the CF model. The sub-population specific time-components $k_t^{(i)}$ is assumed stationary and it described with an order autoregressive $AR(1)$ model:

$$k_t^{(i)} = \phi_0^{(i)} + \phi_1^{(i)} k_{t-1}^{(i)} + o_t^{(i)} \qquad with\ i.i.d\ o_t^{(i)} \sim N(0, (\sigma_o^{(i)})^2) \tag{9}$$

where $\phi_0^{(i)}, \phi_1^{(i)} \in \mathbb{R}, \forall i \in \mathcal{I}$.

2.3. Data

We perform the tests using the ISTAT data. It provides the mortality data of the Italian population for different ages, years and geographic regions. We consider the single-age mortality rates of the total population (male and female together) of full time span available on the ISTAT website[†]. In accordance with the previous notation, we set $\mathcal{X} = \{x \in \mathbb{N}_0 : 0 \leq x \leq 99\}$, $\mathcal{T} = \{t \in \mathbb{N} : 1974 \leq x < 2020\}$. In addition, we focus our attention on the 20 Italian region and set $\mathcal{I} = \{\texttt{Lombardia}, \texttt{Lazio}, \ldots, \texttt{Valle d'Aosta}\}$. A graphical presentation of our dataset is illustrated in Figure 1. It includes some subplots, one for each Italian region, where mortality rates are plotted in log-scale. The order of the subplots reflects the population size of the different regions: the first one refers to Lombardia, that is, the Italian region with the largest population, while the last one refers to Valle d'Aosta, which is the region with the smallest population. Each curve refers to a different calendar year: the curves in the dark blue refer to less recent years while the lighter ones refer to more recent calendar years. It is immediate to note that the most recent curves lie below the dark ones highlighting a progressive decline in mortality for all the 20 Italian regions. Furthermore, we also observe that when one looks at less populated regions, the log-mortality curves exhibit some random fluctuations along the age dimension. This evidence is probably due to the law of large numbers: the estimate of mortality rates is more accurate when measured on large populations such as Lombardia and less precise when a small population such as Valle d'Aosta is considered.

3. Results

This section presents the results of some numerical experiments performed on the ISTAT mortality data.The aim is to analyse and compare the LC, the CF, and the ACF models from different perspectives. The comparison is performed in terms of i) the fitting quality, ii) forecasting accuracy, and iii) the

[†] https://www.istat.it

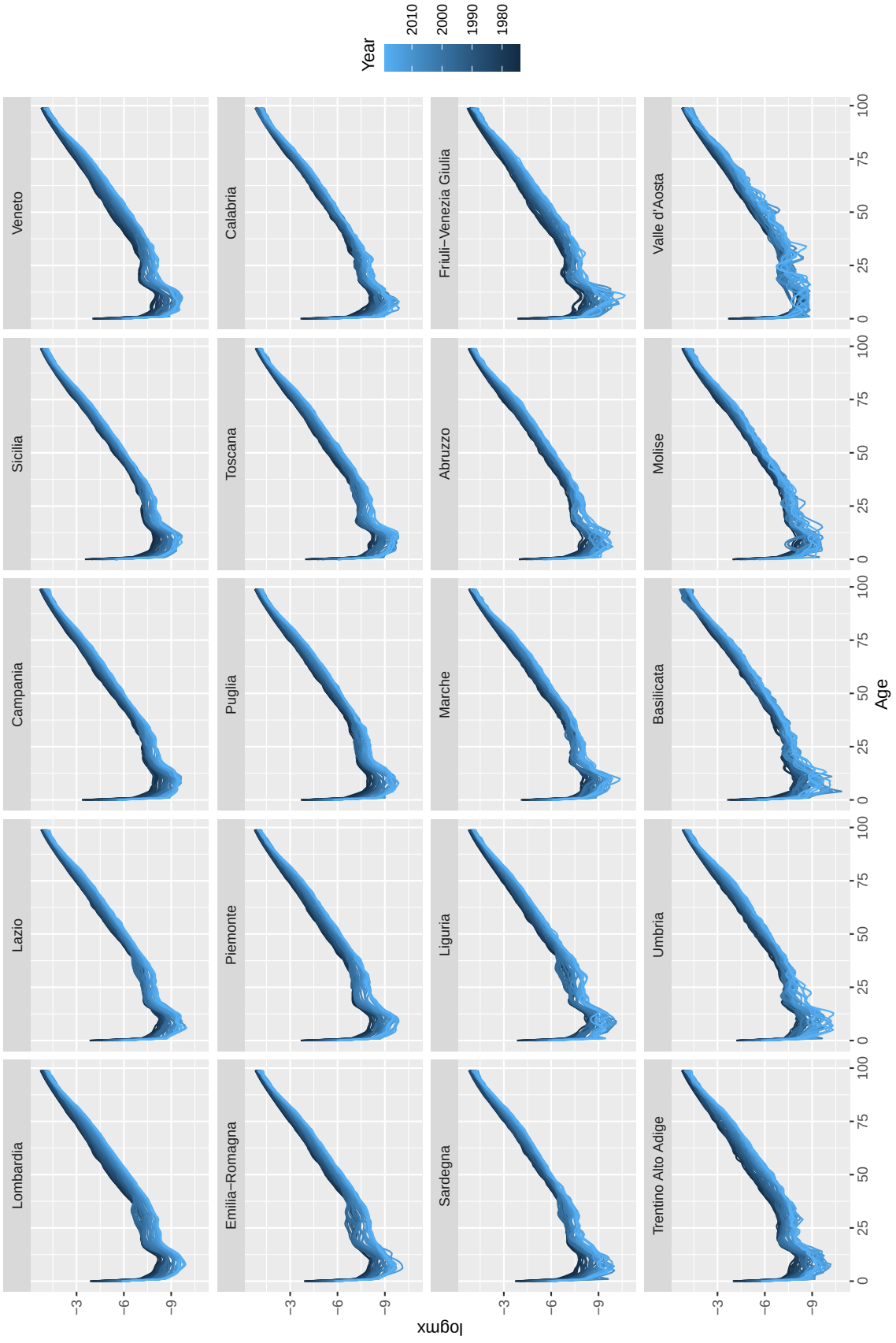

Figure 1. Log-mortality rates in the Italian regions.

number of parameters to optimise. We split the mortality data into two parts. The first set of data consists of the mortality rates for calendar years in $\mathcal{T}_1 = \{t \in \mathcal{T} : t \leq 1999\}$. It is used to fit the models. The second one includes the mortality rates for the calendar years in $\mathcal{T}_2 = \{t \in \mathcal{T} : t > 1999\}$, and it is used to measure the forecasting accuracy of the models.

3.1. Model estimates

First, we discuss the fitting of the LC, CF and ACF models and the resulting estimates. The LC model is estimated individually on the regional data following the SVD-based procedure described in the previous section. Figures 2, 3 and 4 report the estimates of the parameters $(\alpha_x^{(i)})_x$, $(\beta_x^{(i)})_x$ and $(\kappa_t^{(i)})_t$ for the different Italian regions. Also in this case, the order of the subplots reflects the population size of the regions. Analysing Figure 2, we note that the $(\alpha_x^{(i)})_x$ estimates exhibit the classic life table shape for

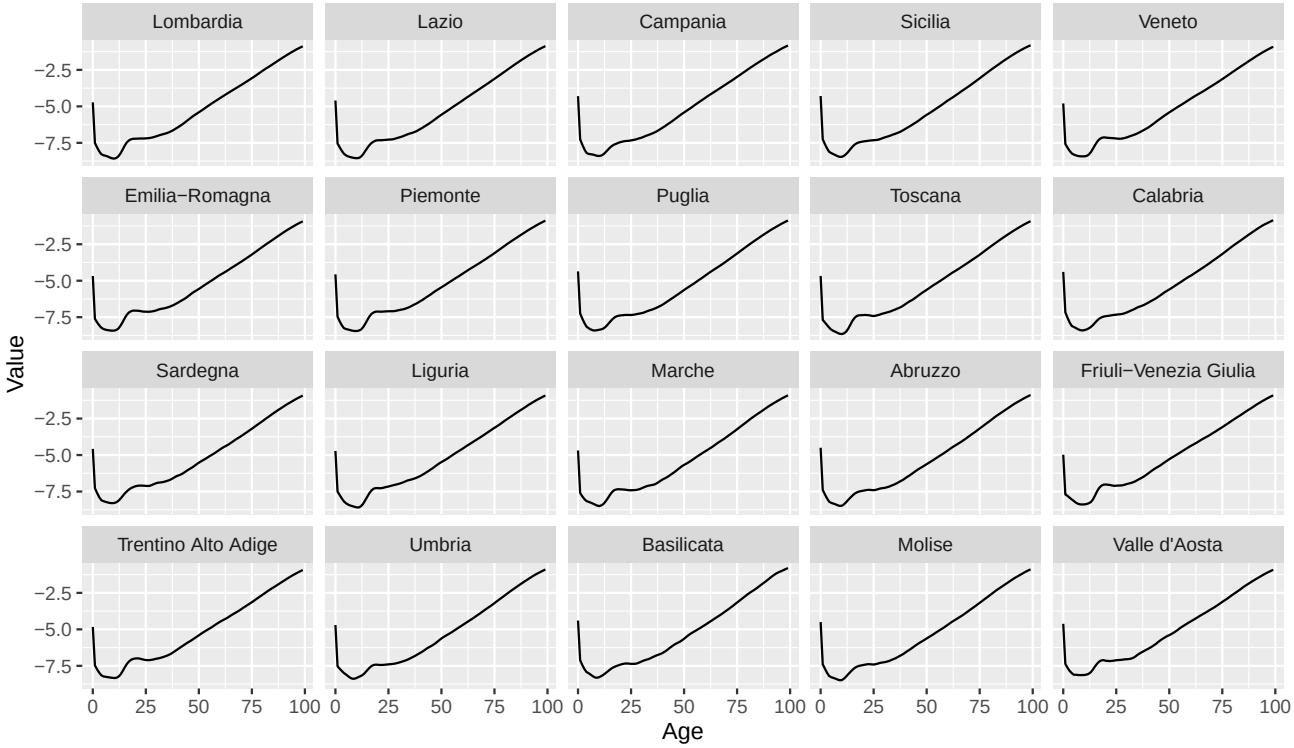

Figure 2. Estimates of $(\alpha_x^{(i)})_x$ of the LC model for the different Italian region.

all the Italian regions, and they are pretty similar among them. In addition, they seem relatively smooth over the age dimension. This result appears reasonable since this curve is estimated as the average of the observed log-mortality rates.

On the contrary, Figure 3 shows that the $(\beta_x^{(i)})_x$ curves present some irregular fluctuations especially for Basilicata and Valle d'Aosta. Unfortunately, this problem is not new to the mortality modelling literature. Delward et al. (2007) argues that an irregular pattern exhibit $(\beta_x^{(i)})_x$ can be observed sometimes and that this issue is undesirable from an actuarial point of view since it could induce erratic variations across ages in the resulting projected life tables. Interestingly, Figure 3 highlights a relationship between the population size and the fluctuation in the $(\beta_x^{(i)})_x$ estimate exists. Indeed, the oscillations appear

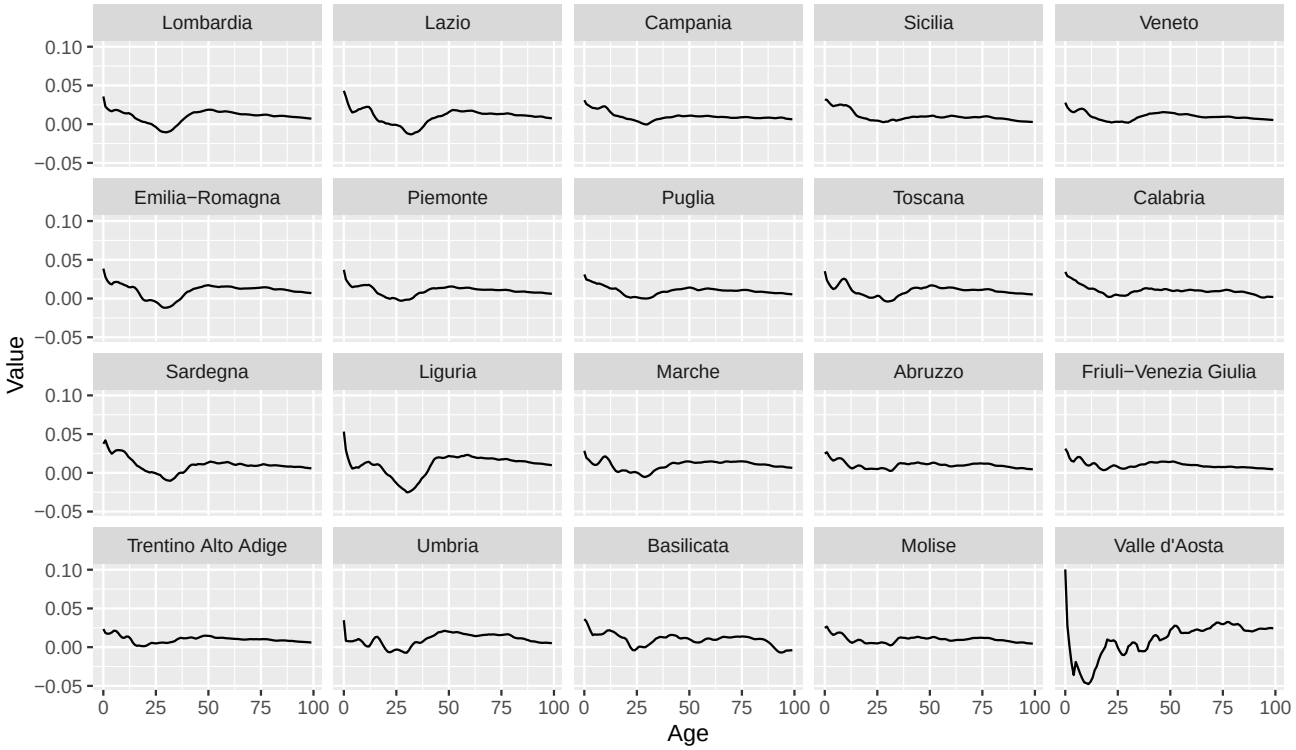

Figure 3. Estimates of $(\beta_x^{(i)})_x$ of the LC model for the different Italian region.

visible for the regions in the bottom of Figure 3 where the low-population[‡] regions are located. One might argue that the use of the LC model may not be adequate for modelling the mortality of regions or subpopulations where the population size is too small. The motivation is due to the law of large numbers. The estimates of the mortality rates are less precise when the sample size decreases. This induces fluctuations in the observed mortality curves and affects the estimates $(\beta_x^{(i)})_x$ estimates, which appear sensitive to this phenomenon.

The $(\kappa_t^{(i)})_t$ estimates for the different regions are presented in Figure 4. A dashed vertical line corresponding to 1999 is drawn. The $(\kappa_t^{(i)})_t$ values on the left of that line are estimated on the mortality data, while the values on the right represent the projections obtained using the ARIMA (0,1,0) models. Figure 4 shows a decreasing trend of the mortality over time, and this evidence confirms that mortality is progressively declining in all Italian regions although the drift terms $\gamma^{(i)}, \forall i \in \mathcal{I}$ appear different. The CF and ACF models are fitted following the procedure described in the original paper and using the same data considered for the LC model. First, the $(B_x^{(i)})_x$ and $(K_t^{(i)})_t$ parameters are estimated by applying the ordinary LC method to the aggregate mortality data. Figure 5 presents the resulting estimates. The $(B_x^{(i)})_x$ curve appears relatively smooth since it is estimated considering the mortality data of all regions. In addition, we also observe that the common risk factor $K(t)$ is downward sloping, implying a long-term trend of mortality improvement in all the Italian regions. Also in this case, the values to the right of the dashed line are the projections obtained via ARIMA (0,1,0) model.

[‡] We use this term to refer to the regions with a small population without considering the geographical extension as it is outside the scope of this research.

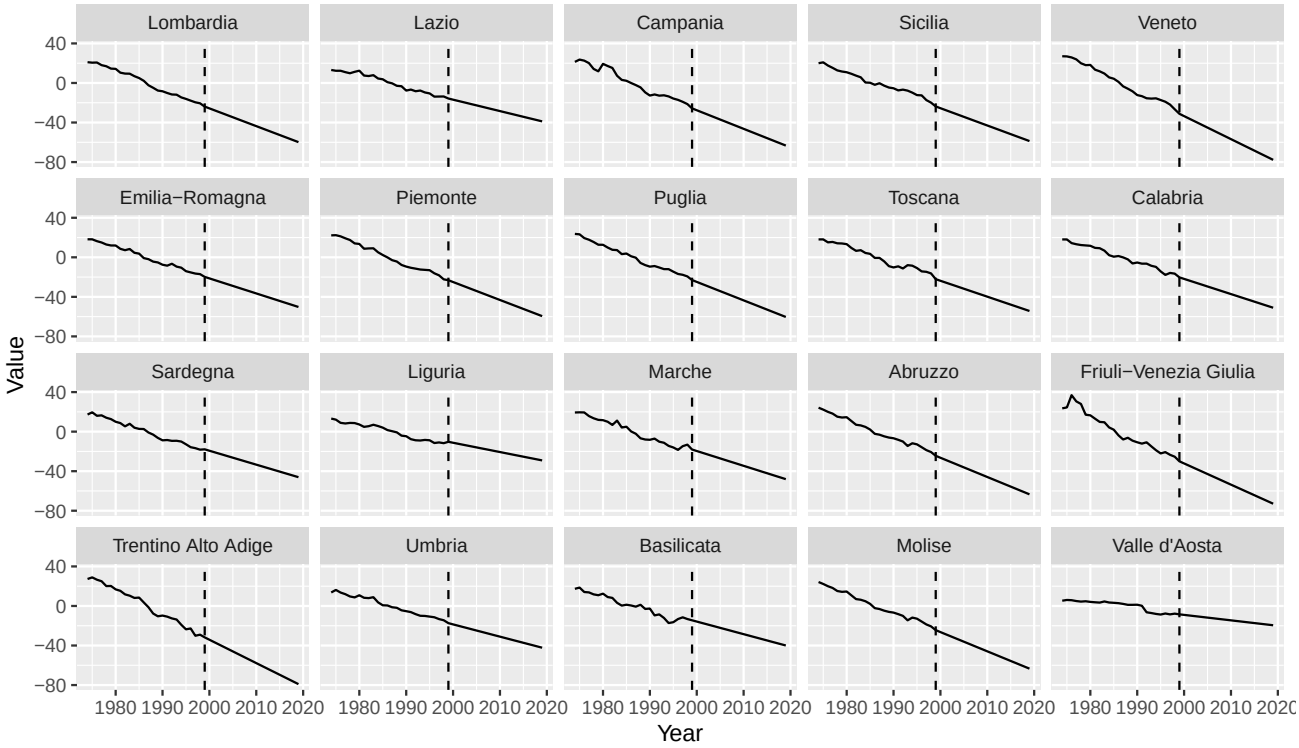

Figure 4. Estimates of $(\kappa_t^{(i)})_t$ of the LC model for the different Italian region.

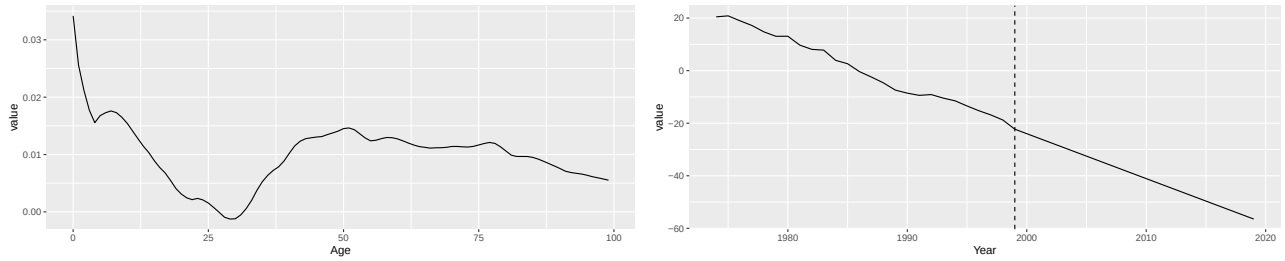

Figure 5. Estimates of $(B_x)_x$ (left) and $(K_t)_t$ (right) of the CF and ACF models.

3.2. Comparison

In this section, some comparisons among the LC, the CF and the ACF models are carried out in terms of fitting quality, forecasting accuracy, and the number of parameters to optimise. The fitting quality and the forecasting accuracy are measured in terms of Mean Squared Error (MSE) and Mean Absolute Error (MAE) of the predicted mortality rates values from the actual ones:

$$MSE = \frac{\sum_x \sum_i \sum_t (\widehat{m}_{x,t}^{(i)} - m_{x,t}^{(i)})^2}{N}$$

$$MAE = \frac{\sum_x \sum_i \sum_t |\widehat{m}_{x,t}^{(i)} - m_{x,t}^{(i)})|}{N}$$

where N is the size of the sample considered. Although the first measure penalises large deviations more than the second one, these two values should be as low as possible. Moreover, we also desire that the

number of parameters fit as low as possible. For this reason, we also analyse the number of parameters and the Bayesian Information (BIC) or Schwarz Criterion. The last one is a measure that considers the fitting quality and the number of parameters required. Models with lower BIC are generally preferred. This criterion is often used in the mortality modelling literature, see Booth et al. (2006); Apicella et al. (2019); Enchev et al. (2017).

Table 1 reports the results LC, CF and ACF models. The MSE and MAE values are in 10^{-4}. We report in bold the best performance for each used criterion.

Table 1. Number of parameters, MSE and MSE for fitting and forecasting of the LC, CF and ACF models; the values are in 10^{-4}.

			Fitting		Forecasting	
Model	# Parameters	BIC	MSE	MAE	MSE	MAE
LC	4560	−99687.64	0.2169	16.2408	2.1162	39.8842
CF	**228**	−99480.93	0.3956	20.1524	4.099	95.0501
ACF	4808	−99718.77	**0.1900**	**15.6569**	**0.7964**	**28.8717**

Intuitively, the CF is the most parsimonious model since it has the lowest number of parameters. The LC model is the second one, while the ACF model is the model that requires the most expensive model in terms of the number of parameters. This ranking changes if we look at the fitting MSE. In particular, we observe that the ACF model obtains the best fitting. The second is the LC model, while the CF model is the least accurate. This evidence continues to hold even if we consider the MAE. This result appears reasonable since more parameters make the model more flexible and, in that case, it should better fit the data points used to optimise the parameters. From a BIC perspective, we observe that the CF model is the best, the LC model the second, and the ACF model the third. This result is probably due to the larger number of parameters required by the ACF model. However, these additional parameters produce a significant gain in forecasting accuracy. The ACF model is the most accurate, the LC model is the second, and the CF model is the least valid. This result is the same for both errors measures.

A more detailed comparison of the fitting and forecasting accuracies is shown in Table 2, which reports the MSE and MAE of the three models in the different Italian regions in the fitting and forecasting. Also in this case, we observe that the CF model is often the least accurate in fitting and forecasting from both MSE and MAE perspectives. The fitting performance of the LC and ACF models are pretty similar: both models achieve the best performance in 50% of the regions considered. This evidence works for both error measures. The ACF model overperforms the LC model from a forecasting point of view. In particular, the ACF model is the best in 75% of cases (15/20) from the MSE point of view, while it has the best performance in 90% of cases (18/20) when the MAE is considered. Furthermore, we observe that the gain in forecasting performance in cases where the LC model overperforms the ACF model (Lazio, Sardegna, Abruzzo) is relatively modest. On the contrary, the gain appears significant in some regions where the ACF model beats the LC model (Lombardia, Calabria, Basilicata). The only case where the LC model overperforms the ACF model from both MAE and MSE perspectives is Toscana. We conclude that the CF model performs poorly on regional Italian data. It is necessary to include the sub-population specific bilinear terms to obtain satisfactory fitting and forecasting performance. We drop the CF model and focus on the LC and ACF models to make further comparisons.

Figure 6 further compares the three methods. It shows the MSE and the MAE in the different

Table 2. MSE and MSE for fitting and forecasting of the LC, CF and ACF models in the different Italian regions; the values are in 10^{-4}.

	Country	LC	CF	ACF	LC	CF	ACF
MSE	Lazio	**0.1570**	0.2493	0.2129	**0.3300**	4.3693	0.3676
	Campania	**0.2504**	0.3694	0.3178	0.9781	4.6704	**0.4238**
	Sicilia	0.2399	0.4170	**0.1117**	1.0505	4.8197	**0.6862**
	Veneto	**0.1192**	0.1884	0.1453	1.4601	3.8790	**0.7292**
	Emilia-Romagna	0.0853	0.1046	**0.0616**	0.9207	3.8268	**0.5885**
	Piemonte	**0.0888**	0.1249	0.0906	0.9305	4.1159	**0.5436**
	Puglia	0.1919	0.2047	**0.1199**	0.4306	4.0716	**0.3730**
	Toscana	0.1161	0.1108	**0.0611**	**0.5179**	4.0900	0.6900
	Calabria	**0.2271**	0.5606	0.3370	3.6670	4.0192	**1.3038**
	Sardegna	**0.1662**	0.1865	0.1696	**0.3854**	3.8333	0.3954
	Liguria	**0.0578**	0.0932	0.0867	**0.3395**	3.8239	0.4457
	Marche	**0.0940**	0.1347	0.1334	0.5868	3.9673	**0.5805**
	Abruzzo	0.0908	0.0845	**0.0767**	**0.3860**	4.2181	0.4180
	Friuli-Venezia Giulia	**0.1282**	0.2029	0.1547	0.6482	3.8721	**0.5260**
	Trentino Alto Adige	**0.1220**	0.3600	0.1314	1.8999	3.7722	**0.8129**
	Umbria	**0.1495**	0.1947	0.1702	0.3939	3.9955	**0.3943**
	Basilicata	1.3531	3.3721	**0.8315**	23.6278	4.2491	**4.2366**
	Molise	0.0908	0.0845	**0.0767**	0.7047	3.9790	**0.6492**
	Valle d'Aosta	0.5261	0.6274	**0.4214**	2.0250	4.6717	**1.4133**
MAE	Lombardia	12.1486	19.9305	**11.7124**	37.2103	92.1732	**26.7736**
	Lazio	**14.5028**	19.4734	18.2472	24.6515	99.9781	**22.3118**
	Campania	**18.7160**	22.9006	20.6232	35.5810	105.6370	**22.8750**
	Sicilia	18.8805	25.5242	**14.3848**	35.0671	105.0941	**28.2108**
	Veneto	**13.3441**	17.9538	14.7495	41.2196	91.4148	**31.1028**
	Emilia-Romagna	12.0344	13.4764	**10.7691**	34.2336	91.4306	**27.3125**
	Piemonte	**11.4615**	13.5049	12.0035	33.6106	96.2467	**27.1122**
	Puglia	16.6614	17.0389	**13.1328**	24.0734	95.4091	**21.9900**
	Toscana	13.9102	14.1957	**11.1923**	**25.4458**	94.1629	28.8530
	Calabria	**17.4076**	27.7452	21.5707	63.3229	95.8088	**33.8510**
	Sardegna	**14.9562**	16.1873	16.2295	26.1191	92.6877	**20.7598**
	Liguria	**11.0432**	13.0582	12.5367	26.6906	93.8239	**24.2515**
	Marche	**12.5060**	13.3978	13.1364	26.7175	91.2184	**26.5269**
	Abruzzo	12.6381	12.3112	**11.4253**	**22.5176**	96.6803	23.4488
	Friuli-Venezia Giulia	**16.4157**	17.1397	16.9118	31.6200	92.1787	**28.2669**
	Trentino Alto Adige	**15.4234**	25.4248	16.1150	45.9268	88.2525	**32.3867**
	Umbria	**16.0213**	18.4215	17.6157	22.9201	93.4483	**22.6744**
	Basilicata	38.5176	58.6050	**31.4198**	164.4508	96.2181	**61.1973**
	Molise	12.6381	12.3112	**11.4253**	28.3012	93.0878	**27.3108**
	Valle d'Aosta	25.5891	24.4487	**17.9363**	48.0054	96.0502	**40.2191**

Figure 6. Forecasting MAE and MSE of the LC, CF and ACF models distinguishing by year.

forecast years from 2000 to 2019. Interestingly, the curves related to the ACF model are the lowest, those relating to the LC model are the second, while the CF model is the least accurate in all forecast years. In the following, we will focus our attention on the LC and ACF model since they are more performing. Figure 7 plots the forecasting error of the LC and ACF models for all ages and calendar years, distinguished by region. The residuals are calculated as predictions minus the observed values, scaled by the estimated standard deviation of the actual values calculated at each age. The red areas in Figure 7 indicate an overestimation of mortality rates, while blue areas indicate an underestimation. Some interesting comments can be made. First, we note that some pronounced red areas are present in the heatmaps related to the LC model for ages 20–45. This result appears especially evident for Liguria, Emilia Romagna, Lombardia and Lazio, highlighting a systematic overestimation of the mortality rates for the LC model in that age range. This effect is less pronounced in the ACF model heatmaps suggesting that it better anticipates longevity improvements and reduces the systematic overestimation of mortality rates at those ages. The overestimation of mortality rates for the LC model also relates to very old ages for some regions; see Basilicata and Calabria. This effect also appears to be less noticeable for the forecasts produced by the ACF model.

Finally, one might also notice that some oblique lines are visible in the heatmaps of both models. This effect, known as the cohort effect, refers to the mortality rates of individuals born in the same year. It is probably because both models don't include cohort terms in the model specification. Figure 8 depicts the confidence intervals at 95% level produced by the LC and ACF models for mortality rates at age $x = 65$. One could observe that the mortality rates of all regions show a decreasing trend suggesting that mortality is improving across all the Italian areas. The ACF model generally presents confidence

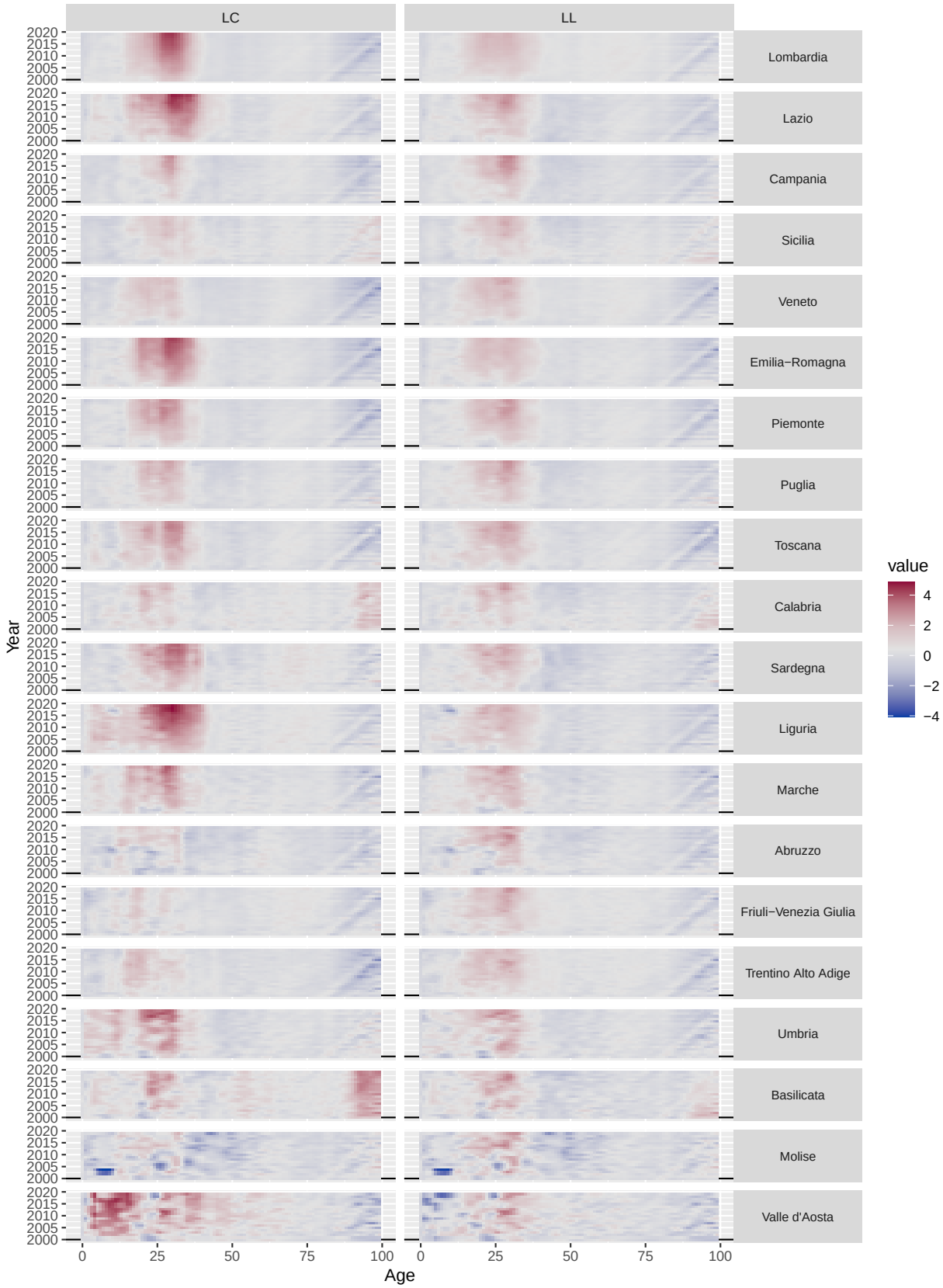

Figure 7. Residuals produced by the LC and ACF models, for each region, year and age.

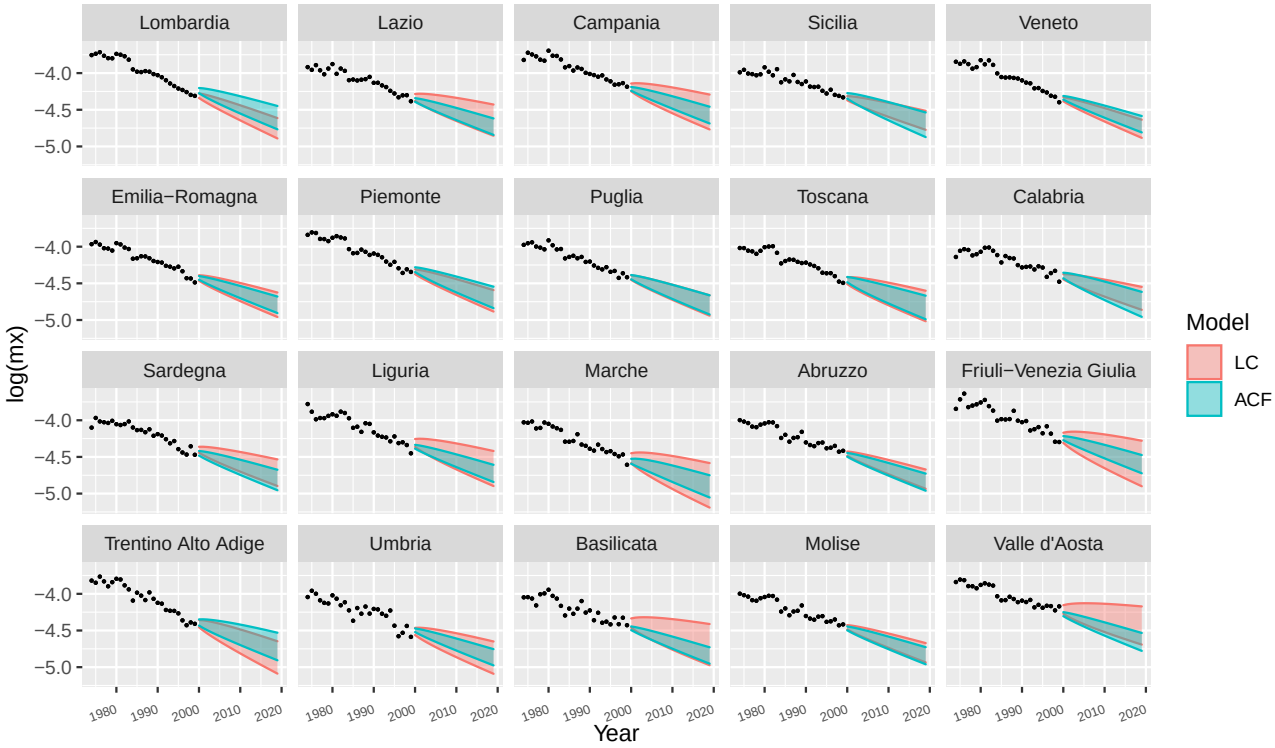

Figure 8. Confidence interval (at 95% level) of the projected log-mortality rates at age $x = 65$ produced by the LC and the ACF models for the different Italian region.

intervals of similar width for all regions. In contrast, the LC model generates narrowed confidence bands for high-population regions such as Lombardia and Lazio and wide confidence bands for low-population regions such as Valle d'Aosta and Basilicata. Furthermore, we observe that in some regions, such as Abruzzo, Molise, Puglia, Piemonte, and Veneto, the confidence intervals produced by the two models are quite similar, while they appear different for Valle d'Aosta and Basilicata.

Figure 9 presents the projected log mortality curves obtained via LC and ACF models for t = 2000, 2010, 2020, 2030, and different Italian regions. The ACF model produces coherent forecasts since the projected curves do not diverge in the long run. In contrast, the projections obtained via single-population LC models diverge when t increases.

4. Application to the Annuity value

In this section, we measure the impact of applying the regional mortality data and the ACF model to evaluate life annuity. The price of an immediate life annuity sold to an individual aged x in year t is given by:

$$a_{x,t} = \sum_{k\geq 0}\{\prod_{j=0}^{k} p_{x+j,t+j}\}(1+r)^{-(k+1)}$$

where $p_{x,t}$ is the one-year survival probability derived from the mortality model, and r is the interest rate. The annuity value is a random variable, and simulation-based approaches are often used to compute

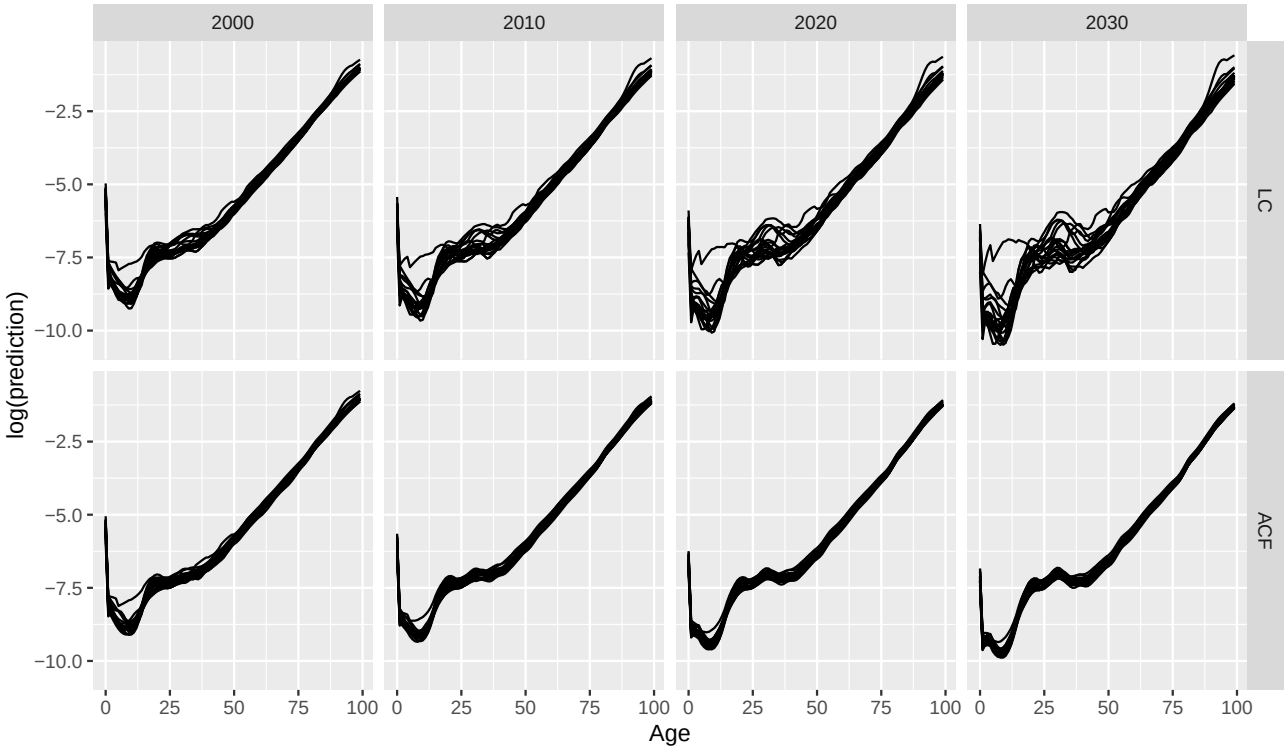

Figure 9. Projected log-mortality curves of the LC ACF models for $t = 2000, 2010, 2020, 2030$.

its distribution. In this case, we consider the interest rate as deterministic, while the mortality risk is stochastic. We derive the distribution of value of an immediate life annuity with $x = 65$ and $t = 1999$ for each Italian region, simulating possible trajectories of the future mortality evolution according to the ACF model. In this case, we consider only the random error of projecting the mortality indices K_t and $\kappa_t^{(i)}$ as risk sources. A sample of 10000 paths is generated, and the resulting annuity values are computed. The interest rate is assumed to be equal to zero; therefore, $a_{x,t}$ corresponds to the life expectancy at age x and time t. Figure 10 shows the simulated distributions of the annuity price for all the Italian regions. We also report the value of an immediate life annuity computed according to the LC model using the total national data. This value represents an interesting benchmark since annuity pricing is generally performed using national data as also discussed in Bozzo et al. (2021). It is denoted with a vertical red line in Figure 10. For this national benchmark, we use Human Mortality Database (HMD) dataWilmoth & Shkolnikov (2021). [§] We observe some heterogeneity in the distributions of the different regions. In some cases, the (average) annuity value difference is almost equal to 2 years (see Marche and Sicilia). This evidence had already been observed, in terms of average values, in Bozzo et al. (2021). In particular, Figure 10 shows that the distributions of the annuity value for some regions are essentially below the national average (See Sicilia and Campania) and vice versa, there are some regions where the annuity value is above the reference value (Marche). Some differences are also visible in the variability: Molise and Abruzzo have more concentrated distributions around the average, while

[§] It is the most popular data source for the study of mortality and provides data at the national level (rates, deaths, exposure to risk) for a large set of countries and calendar years. We calibrate the LC model employing the same period and age range described above.

Sicily and Trentino have more dispersed distributions. In general, Figure 10 highlights a certain degree of heterogeneity across the different Italian regions. This result points out the importance of considering differences in mortality among the Italian regions in the actuarial calculations.

5. Conclusions

This paper presents a comparison of different approaches to modelling Italian sub-national mortality data. We consider the independent modelling approach based on rdsingle-population LC models and the coherent multi-population model proposed by Li & Lee (2005). The analysis was performed on the Italian mortality data provided at the regional level by ISTAT. The tests have shown that, although the two models produce somewhat similar fitting performance, the ACF model produces significantly better forecasting performances. It beats the LC model in 90% of the Italian regions from an MAE perspective. In addition, the ACF model appears to capture and predict longevity improvements better. The ACF model was also employed to simulate the annuity prices of an individual aged 65 in 1999 in the different Italian regions. We observed some heterogeneity among the regions. Furthermore, in some cases, the value of the annuity differed significantly from the national benchmark. The analysis of the regional data could provide additional information about the heterogeneity in longevity in the national population. In particular, understanding the regions' mortality differences could be helpful from a longevity risk management perspective. Indeed, suppose an annuity portfolio that is not adequately balanced between annuitants living in areas characterised by higher life expectancies and annuitants residing in regions with lower life expectancy. In that case, the use of aggregate national data could lead to misestimating future liabilities and inducing financial trouble. Future research will proceed in different ways. First, we plan to investigate sub-national data of other countries like the United States, Hungary and France. Second, we would like to explore the application of more sophisticated single-population and multi-population mortality models Kleinow (2015); Hyndman et al. (2013). The use of non-linear mortality models could highlight further interesting information on the difference in subnational mortality data. Finally, we aim to explore the use of machine learning and deep learning techniques in sub-national mortality data, which have shown enormous potential in multi-country and large-scale mortality modelling; see for example Perla et al. (2021); Richman & Wüthrich (2021).

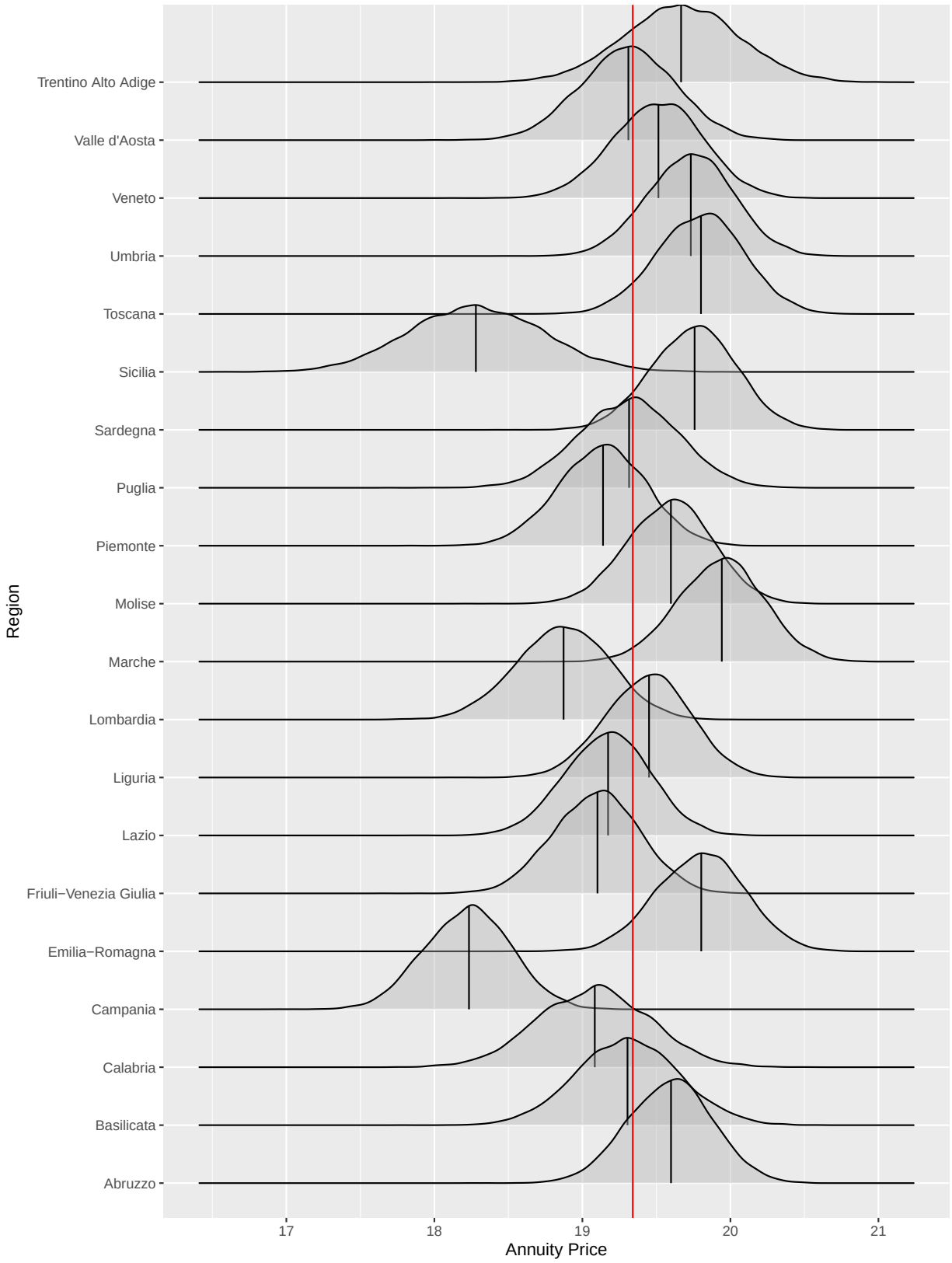

Figure 10. Random present value of an immediate life annuity with $x = 65$ and $t = 1999$ for each Italian region according to the ACF model.

Acknowledgements

The author thank the three anonymous referees for helpful comments that greatly improved the article.

Conflict of interest

The author declares no conflict of interest in this paper.

References

Apicella G, Dacorogna M, Di Lorenzo E, et al. (2019) Improving the forecast of longevity by combining models. *N Am Actuar J* 23: 298–319. https://doi.org/10.1080/10920277.2018.1556701

Booth H, Hyndman RJ, Tickle L, et al. (2006) Lee-Carter mortality forecasting: a multi-country comparison of variants and extensions. *Demogr Res* 15: 298–319. https://doi.org/10.4054/DemRes.2006.15.9

Bozzo G, Levantesi S, Menzietti M (2021) Longevity risk and economic growth in sub-populations: evidence from Italy. *Decis Econ Financ* 44: 101–115. https://doi.org/10.1007/s10203-020-00275-x

Brouhns N, Denuit M, Vermunt JK (2002) A Poisson log-bilinear regression approach to the construction of projected lifetables. *Insur Math Econ* 31: 373–393. https://doi.org/10.1016/S0167-6687(02)00185-3

Cairns A, Blake D, Dowd K (2006) A two-factor model for stochastic mortality with parameter uncertainty: theory and calibration. *J Risk Insur* 73: 687–718. https://doi.org/10.1016/S0167-6687(02)00185-3

Cairns A, Blake D, Dowd K, et al. (2009) A quantitative comparison of stochastic mortality models using data from England and Wales and the United States. *N Am Actuar J* 13: 1–35. https://doi.org/10.1080/10920277.2009.10597538

Chen H, MacMinn R, Sun T (2015) Multi-population mortality models: A factor copula approach. *Insur Math Econ* 63: 135–146. https://doi.org/10.1016/j.insmatheco.2015.03.022

Chen RY, Millossovich P (2018) Sex-specific mortality forecasting for UK countries: a coherent approach. *Eur Actuar J* 8: 69–95. https://doi.org/10.1007/s13385-017-0164-0

Currie ID (2013) Smoothing constrained generalized linear models with an application to the Lee-Carter model. *Stat Model* 13: 69–93. https://doi.org/10.1177/1471082X12471373

Currie ID, Durban M, Eilers PHC (2018) Smoothing and forecasting mortality rates. *Stat Model* 4: 279–298. https://doi.org/10.1191/1471082X04st080oa

Danesi IL, Haberman S, Millossovich P (2018) Forecasting mortality in subpopulations using Lee–Carter type models: A comparison. *Insur Math Econ* 62: 151–161. https://doi.org/10.1016/j.insmatheco.2015.03.010

Delwarde A, Denuit M, Eilers P (2007) Smoothing the Lee–Carter and Poisson log-bilinear models for mortality forecasting: a penalized log-likelihood approach. *J Popul Res* 7: 29–48. https://doi.org/10.1177/1471082X0600700103

De Waegenaere A, Melenberg B, Stevens R (2010) Longevity risk. *De Econ* 158: 151–192. https://doi.org/10.1007/s10645-010-9143-4

Enchev V, Kleinow T, Cairns A (2017) Multi-population mortality models: fitting, forecasting and comparisons. *Scand Actuar J* 4: 319–342. https://doi.org/10.1080/03461238.2015.1133450

Franzini L, Giannoni M (2010) Determinants of health disparities between Italian regions. *BMC Public Health* 10: 1–10. https://doi.org/10.1186/1471-2458-10-296

Gao G, Shi Y (2021). Age-coherent extensions of the Lee–Carter model. *Scand Actuar J* 10: 998–1016. https://doi.org/10.1080/03461238.2021.1918578

Hainaut D, Denuit M (2020) Wavelet-based feature extraction for mortality projection. *ASTIN B J IAA* 50: 675–707. https://doi.org/10.1017/asb.2020.18

Hyndman RJ, Ullah MS (2007) Robust forecasting of mortality and fertility rates: A functional data approach. *Comput Stat & Data Anal* 51: 4942–4956. https://doi.org/10.1016/j.csda.2006.07.028

Hyndman R, Booth H, Yasmeen F (2017) Coherent mortality forecasting: the product-ratio method with functional time series models. *Demography* 50: 261–283. https://doi.org/10.1007/s13524-012-0145-5

Kleinow T (2015) A common age effect model for the mortality of multiple populations. *Insur Math Econ* 63: 147–152. https://doi.org/10.1007/s13524-012-0145-5

Lee RD, Carter LR (1992) Modeling and forecasting US mortality. *J Am Stat Assoc* 87: 659–671. https://doi.org/10.1080/01621459.1992.10475265

Li N, Lee R (2005) Coherent mortality forecasts for a group of populations: An extension of the Lee-Carter method. *Demography* 42: 575–594. https://doi.org/10.1353/dem.2005.0021

Li J (2013) A Poisson common factor model for projecting mortality and life expectancy jointly for females and males. *Popul Stud* 67: 111–126. https://doi.org/10.1080/00324728.2012.689316

Nigri A, Levantesi S, Marino M, et al. (2019) A deep learning integrated Lee–Carter model. *Risks* 7: 33. https://doi.org/10.3390/risks7010033

Perla F, Richman R, Scognamiglio S, et al. (2021) Time-series forecasting of mortality rates using deep learning. *Scand Actuar J* 2021: 1–27. https://doi.org/10.1080/03461238.2020.1867232

Renshaw A, Haberman S (2003) Lee–Carter mortality forecasting with age-specific enhancement. *Insur Math Econ* 33: 255–272. https://doi.org/10.1016/S0167-6687(03)00138-0

Renshaw A, Haberman S (2006) A cohort-based extension to the Lee–Carter model for mortality reduction factors. *Insur Math Econ* 38: 556–570. https://doi.org/10.1016/j.insmatheco.2005.12.001

Richman R, Wüthrich MV (2021) A neural network extension of the Lee–Carter model to multiple populations. *Ann Actuar Sci* 15: 346–366. https://doi.org/10.1017/S1748499519000071

Schnürch S, Kleinow T, Korn R (2021) Clustering-Based Extensions of the Common Age Effect Multi-Population Mortality Model. *Risks* 9: 45. https://doi.org/10.3390/risks9030045

Shang HL, Yang Y (2021) Forecasting Australian subnational age-specific mortality rates. *J Popul Res* 38: 1–24. https://doi.org/10.1007/s12546-020-09250-0

Wilmoth JR and Shkolnikov V (2021) University of California, Berkeley (US), and Max Planck Institute for Demographic Research (Germany).

AIMS Press